Acta Crystallographica Section D
Biological Crystallography
ISSN 0907-4449

Structural phase transition of monoclinic crystals of hen egg-white lysozyme

Kazuaki Harata* and Toshihiko Akiba

Biological Information Research Center, National Institute of Advanced Industrial Science and Technology (AIST), Central 6, 1-1-1 Higashi, Tsukuba, Ibaraki 305-8566, Japan

Correspondence e-mail: k-harata@aist.go.jp

Received 21 October 2005
Accepted 12 January 2006

PDB References: hen egg-white lysozyme, crystal type IA, 2d4i, r2d4isf; crystal type IB, 2d4j, r2d4jsf; crystal type IIA, 2d4k, r2d4ksf.

Two monoclinic crystals (space group $P2_1$) of hen egg-white lysozyme, a type I crystal grown at room temperature in a D_2O solution with pD 4.5 containing 2%(*w*/*v*) sodium nitrate and a type II crystal grown at 313 K in a 10%(*w*/*v*) sodium chloride solution with pH 7.6, were each transformed into another monoclinic crystal with the same space group by dehydration-induced phase transition. Changes in X-ray diffraction were recorded to monitor the progress of the crystal transformation, which started with the appearance of diffuse streaks. In both crystals, the intensity of $h + l$ odd reflections gradually weakened and finally disappeared on completion of the transformation. X-ray diffraction in the intermediate state indicated the presence of lattices of both the native and transformed crystals. In the native type I crystal, two alternate conformations were observed in the main chain of the region Gly71–Asn74. One conformer bound a sodium ion which was replaced with a water molecule in the other conformer. In the transformed crystal, the sodium ion was removed and the main-chain conformation of this region was converted to that of the water-bound form. The transformed crystal diffracted to a higher resolution than the native crystal, while the peak width of the diffraction spots increased. Analysis of the thermal motion of protein molecules using the TLS model has shown that the enhancement of the diffraction power in the transformed crystal is mainly ascribable to the suppression of rigid-body motion owing to an increase in intermolecular contacts as a result of the loss of bulk solvent.

1. Introduction

Protein crystals contain large amounts of solvent, mostly making up 30–70%(*v*/*v*) of the crystal volume (Matthews, 1968). Protein molecules are surrounded by solvent and their packing arrangement is retained by limited intermolecular contacts, which include hydrogen bonds, salt linkages, van der Waals contacts *etc.* A change in the crystal environment first affects the bulk solvent that fills the intermolecular space, with consequent changes in the crystal structure. Protein crystals in controlled humidity environments showed a large change in unit-cell parameters and X-ray diffraction images when the humidity was decreased (Kiefersauer *et al.*, 2000; Dobrianov *et al.*, 2001; Sjögren *et al.*, 2002). When a protein crystal is slowly and carefully dehydrated, it is in a metastable state in the early stage in which the crystal still retains the original packing structure (Dobrianov *et al.*, 1999). Further dehydration causes collapse of the crystal lattice: the crystal no longer maintains its packing structure because of the loss of a large amount of bulk solvent. In some crystals, however, the dehydration induces molecular rearrangement, which transforms the

crystal into a new crystal that is stable and has a lower solvent content.

A phase transition of protein crystals mediated by dehydration was first observed in a monoclinic crystal of hen egg-white lysozyme (Salunke *et al.*, 1985). In addition to the lysozyme crystal, the structures of several dehydrated protein crystals with various solvent contents have been investigated and the structural changes have been discussed in relation to the change in solvation (Kodandapani *et al.*, 1990; Madhusudan *et al.*, 1993; Kishan *et al.*, 1995; Esnouf *et al.*, 1998; Bell, 1999). However, no attempt had been made to elucidate the mechanism underlying the phase transition of protein crystals until we succeeded in measuring the X-ray diffraction of the intermediate state (Harata & Akiba, 2004). In the present paper, we report the X-ray diffraction study of the phase transition of monoclinic lysozyme crystals. We used two types of monoclinic crystals, designated type I (Nagendra *et al.*, 1996) and type II (Harata, 1994), which were obtained under different crystallization conditions. The thermal motion of protein molecules in the crystalline state was analyzed using the TLS model (Schomaker & Trueblood, 1968) to elucidate the origin of the enhancement of the diffraction power of the transformed crystal.

Table 1
Crystallographic data and summary of structure determination.

Values in parentheses are for the last resolution shell.

	Crystal IA (before transition)	Crystal IB (after transition)	Crystal IIA (before transition)	Crystal IIB (after transition)
Crystal data				
Space group	$P2_1$	$P2_1$	$P2_1$	$P2_1$
Unit-cell parameters				
a (Å)	28.01	26.46	27.22	26.83
b (Å)	62.92	58.18	63.48	60.98
c (Å)	60.49	30.85	59.19	31.30
β (°)	90.6	111.3	92.9	111.4
V_M (Å^3 Da^{-1})	1.84	1.53	1.76	1.64
Data collection				
Temperature (K)	290	290	290	
Resolution range (Å)	17.2–1.13 (1.17–1.13)	12.3–1.16 (1.20–1.16)	19.7–1.15 (1.17–1.15)	
Observed data	129895 (6095)	68317 (3043)	277299 (10613)	
Unique data	68963 (4445)	25242 (1587)	67029 (2468)	
R_{merge}	0.067 (0.415)	0.106 (0.299)	0.119 (0.336)	
Completeness (%)	88.7 (57.3)	83.6 (52.8)	93.9 (62.2)	
Structure refinement				
No. of reflections	66282 (6959)	25218 (2638)	66976 (7007)	
No. of parameters	20956	10393	20640	
Resolution range (Å)	17.2–1.16 (1.22–1.16)	12.3–1.16 (1.23–1.16)	19.7–1.15 (1.20–1.15)	
R (all data)	0.136 (0.376)	0.097 (0.169)	0.132 (0.331)	
R_{free} (5% of data)	0.175	0.133	0.164	
Contents of the ASU				
Protein molecules	2	1	2	
Sodium ions	1		2	
Nitrate ions	5	4		
Chloride ions			2	
Water sites	237	129	251	
Average coordinate error (Å)				
Main-chain atoms	0.020	0.014	0.017	
All atoms	0.034	0.025	0.028	

2. Materials and methods

2.1. Preparation of crystals

The type I crystal with space group $P2_1$ was obtained at room temperature from a D_2O solution, since D_2O has been found to be a good solvent for preparing high-quality protein crystals (Harata *et al.*, 1999). 100 mg lyophilized protein (Seikagaku Kogyo Co.) was dissolved in 10 ml D_2O solution with pD 4.5 containing 2%(*w*/*v*) $NaNO_3$ and 50 m*M* sodium acetate. The pD of the protein solution was adjusted to 4.5 with 1 *N* acetic acid. The solution was passed through a 0.2 µm filter and divided into 1 ml portions in small culture dishes, which were allowed to stand in a sealed container. Rod-like crystals grew over two weeks at room temperature. The type II crystal with the same space group was prepared according to a previously reported method (Harata, 1994).

2.2. X-ray measurement

X-ray experiments were carried out on a Bruker Smart6000 diffractometer equipped with a MacScience M06X rotating-anode generator (50 kV, 90 mA) and Osmic Confocal Max-Flux Optics. The intensity data of the native crystal were measured at 290 K using a crystal sealed in a glass capillary with a drop of mother solvent. To measure the phase transition, a type I crystal was immersed in paraffin oil and visible solvent was carefully removed. The crystal in an oil drop was picked up using a cryoloop (Hampton Research) and placed into a nitrogen-gas stream at 273 K on the diffractometer. The orientation of the crystal was roughly adjusted so that the *a* axis was almost parallel to the incident X-ray beam. The change in the X-ray diffraction was recorded every 5 min with an exposure time of 30 s for 1° rotation. When the phase transition was finished, the nitrogen-gas stream was stopped and the intensity data for the structure determination were collected at 290 K. The phase transition of the type II crystal was measured using a crystal in an open glass capillary in a nitrogen-gas stream at 273 K. The X-ray diffraction was recorded using the same procedure as used in the measurement of the type I crystal.

2.3. Structure determination

The structures of the native and transformed crystals were determined by molecular replacement using the atomic coordinates of corresponding structures deposited with the Protein Data Bank [1lj4 for the type I crystal (Nagendra *et al.*, 1996), 1xek for the transformed crystal (Nagendra *et al.*, 1998) and 1lys for the type II crystal (Harata, 1994)]. In the structure

refinement using *SHELX*97 (Scheldrick, 1997), the H-atom coordinates were calculated and included in the structure-factor calculation with an isotropic temperature factor that was 1.2 or 1.5 times larger than that of bonded non-C or C atoms, respectively. Electron-density peaks higher than 0.25 e Å^{-3} were considered to be solvent atoms. Two solvent peaks with a distance of less than 2.5 Å were treated as disorder. After solvent molecules had been picked and disordered side-chain groups had been reasonably modelled, the block-matrix least-squares calculation was adopted for two protein molecules and a set of solvent molecules in the native type I and type II crystals. For the transformed crystal, the full-matrix least-squares calculation was adopted at the final stage. The statistics of data collection and structure refinement are given in Table 1.

2.4. Analysis of rigid-body motion

The rigid-body motion of lysozyme molecules was analyzed to evaluate the characteristics of the thermal motion of protein molecules in the native and transformed crystals using the TLS model (Schomaker & Trueblood, 1968), which represents rigid-body motion as a linear combination of the translational motion (T), librational motion (L) and screw motion (S). Each term of the anisotropic temperature factor, u_{ij}, is expressed as follows:

$$u_{ij} = \sum G_{ijkl} L_{kl} + \sum H_{ijkl} S_{kl} + T_{ij},$$

where G_{ijkl} and H_{ijkl} are functions of the atomic coordinates. The tensor matrices L_{kl}, S_{kl} and T_{ij} were determined by least-squares fit to the observed u_{ij}. The centre of rotation was determined so that the S_{kl} matrix was symmetrical. Atomic thermal motion consists of rigid-body motion and internal motion, which is the fluctuation of the protein structure. The contribution of the rigid-body motion was estimated according to a previously reported method (Harata *et al.*, 1999).

3. Results

3.1. X-ray measurement of the phase transition

The monoclinic type I crystal of hen egg-white lysozyme was transformed into another monoclinic crystal by the loss of 41%(v/v) of the solvent in the crystal. Fig. 1 shows the crystal packing of the native crystal and that of the transformed crystal. While the native type I crystal with 33.2%(v/v) solvent content contains two protein molecules in the asymmetric unit, the transformed type I crystal contains one molecule in the asymmetric unit and the solvent content is only 19.6%(v/v). The start of the phase transition was detected by the appearance of diffuse streaks and an increase in the peak width of the diffraction spots. As shown in Fig. 2, as the transformation of the crystal progressed the intensity of $h + l$ odd reflections decreased and the transformation was completed when these reflections disappeared. It is noteworthy that the diffraction power of the crystal was markedly increased after the phase transition. In Fig. 2, diffraction spots of the native crystal are visible to 1.4 Å resolution. In contrast, the transformed crystal diffracts beyond 1.2 Å resolution, while the peak width of the diffraction spots increases.

The type II crystal with 30.1%(v/v) solvent content was more stable towards dehydration than the type I crystal; the phase transition did not occur in 24 h under the conditions used for the type I crystal. The type II crystal was then placed in an open glass capillary and slowly dehydrated in a 273 K nitrogen-gas stream. The change in the X-ray diffraction images recorded using the same procedure used to measure the type I crystal indicated that the phase transition of the type II crystal progressed similarly to that of the type I crystal. The transformed crystal diffracted to a resolution of higher than 1.2 Å. The unit-cell parameters of the transformed crystal indicate that the shrinkage of the unit cell was less than that of the type I crystal. The solvent content of the transformed crystal was 25.0%(v/v) and the solvent loss was 17%.

3.2. Structure of the native crystal

In the both type I and type II crystals the asymmetric unit contains two protein molecules. Nitrate and chloride ions are mostly located at sites where anions are frequently observed in lysozyme crystals (Vaney *et al.*, 2001). Molecule 1 is roughly related to molecule 2 by the translation $x' = x + 1/2$ and $z' = z + 1/2$ as shown in Fig. 1. The backbone structures of the two molecules in the type I crystal superimpose with a root-mean-square difference of 0.40 Å for equivalent C$^{\alpha}$ atoms,

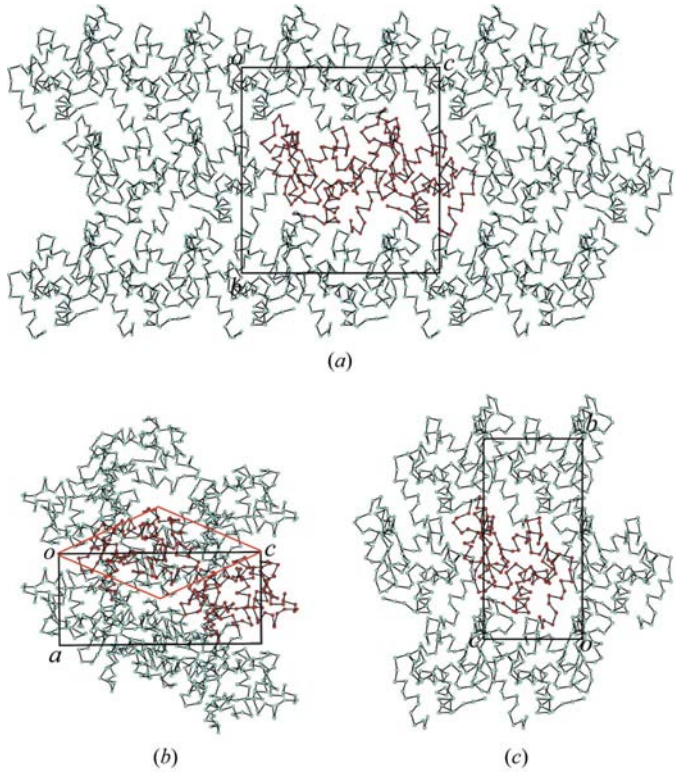

Figure 1
The crystal packing of the type I native crystal viewed along the a axis (a) and along the b axis (b) and the transformed type I crystal viewed along the a axis (c). Independent molecules are shown in red. A unit cell corresponding to that of the transformed crystal is shown by red lines in (b).

except for the region Gly71–Asn74 of molecule 2, which shows two alternate conformations. The disorder of the Gly71–Asn74 region is coupled with the binding of a sodium ion as shown in Fig. 3. In one conformer, a sodium ion is bound to the centre of the large helical loop including the disordered region. Six O atoms from the peptide groups of Ser60, Cys64 and Arg73, a water molecule and a nitrate ion are coordinated to the sodium ion to form a distorted octahedral structure. The structure of the Gly71–Asn74 region of the other conformer is the same as that of the corresponding region in molecule 1, where the sodium and nitrate ions are replaced by water molecules. In the sodium-bound structure, the O atom of the peptide group linking Arg73 and Asn74 is coordinated to the sodium ion. In contrast, the corresponding peptide group in the water-bound structure is rotated by 180° and the amino group is hydrogen-bonded to a water molecule. The crystal

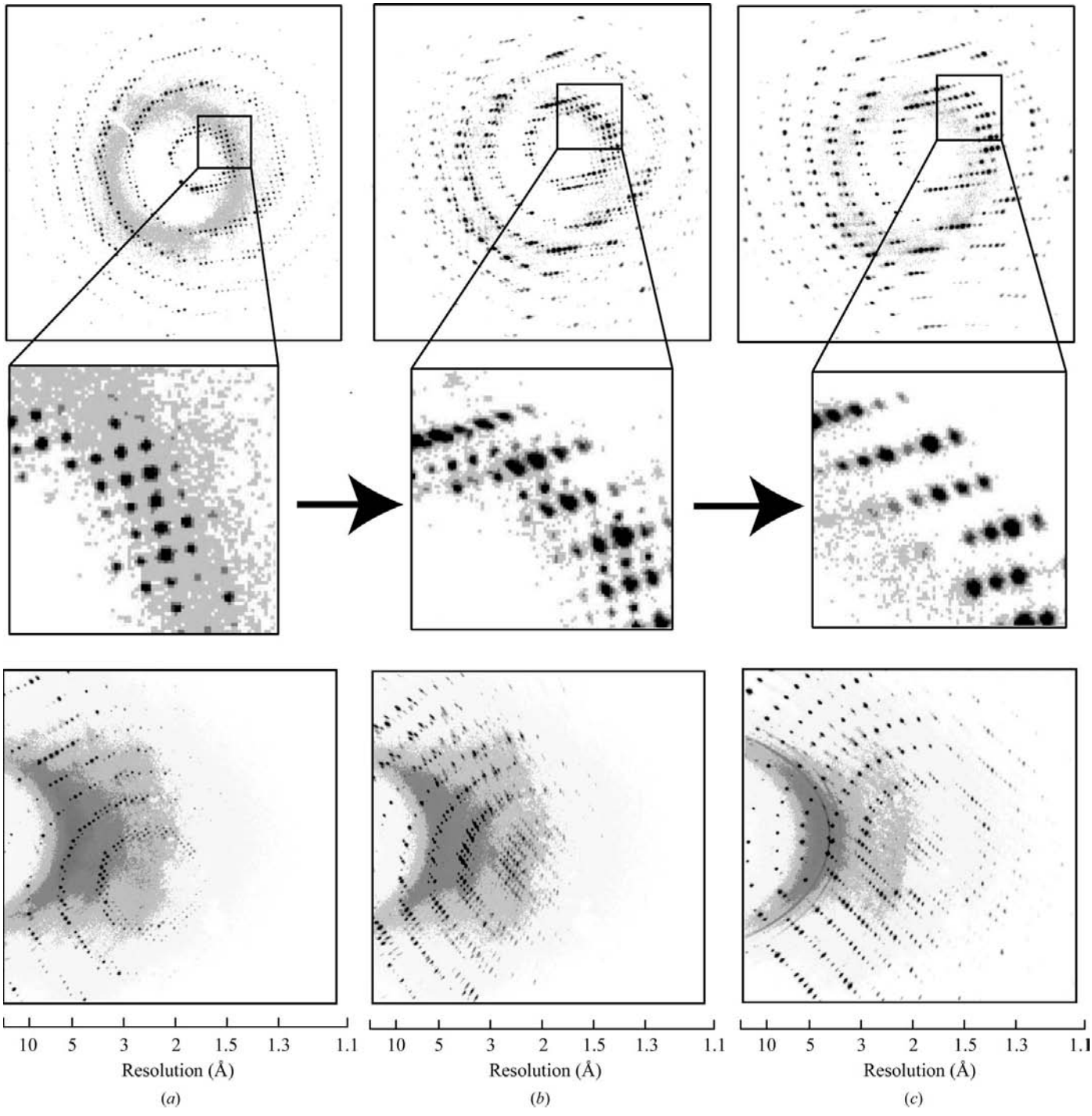

Figure 2
X-ray diffraction images of the type I crystal: native crystal (*a*), intermediate state of the phase transition (*b*) and transformed crystal (*c*). The crystal was roughly adjusted with the *b***c** plane perpendicular to the incident X-ray.

packing of the type II crystal is nearly same as that of the type I crystal. The sodium ion is fully bound to the sodium-binding site in both independent molecules.

3.3. Structure of the transformed crystal

The asymmetric unit contains one protein molecule. The calculated crystal density of 1.24 g cm^{-3} indicates that most solvent molecules are accounted for in the refined structure. The backbone structure is essentially the same as that of molecule 1 in the type I crystal, as indicated by the root-mean-square difference of equivalent C^{α} atoms of 0.47 Å. No sodium ion is observed in the large loop region that includes residues Gly71–Asn74. The protein molecules in the transformed crystal are more densely packed than those in the native crystal. The intermolecular space filled with solvent in the native crystal is reduced in the transformed crystal, as shown in Fig. 4. The side-chain group of Arg114 located on the molecular surface is surrounded by solvent in the native crystal and makes no intermolecular contacts except for a hydrogen-bonding contact with the main-chain O atom of Lys13 in molecule 1. In contrast, the solvent area surrounding Arg114 is so reduced in the transformed crystal that Arg114 can form hydrogen bonds with the main-chain O atoms of Gly16 and Asp18 and a salt linkage with the carboxyl group of Asp18. Fig. 5 shows the changes in the environment surrounding Trp62. In molecule 1 of the native crystal, the disordered side chain of Trp62 is mostly exposed to the bulk

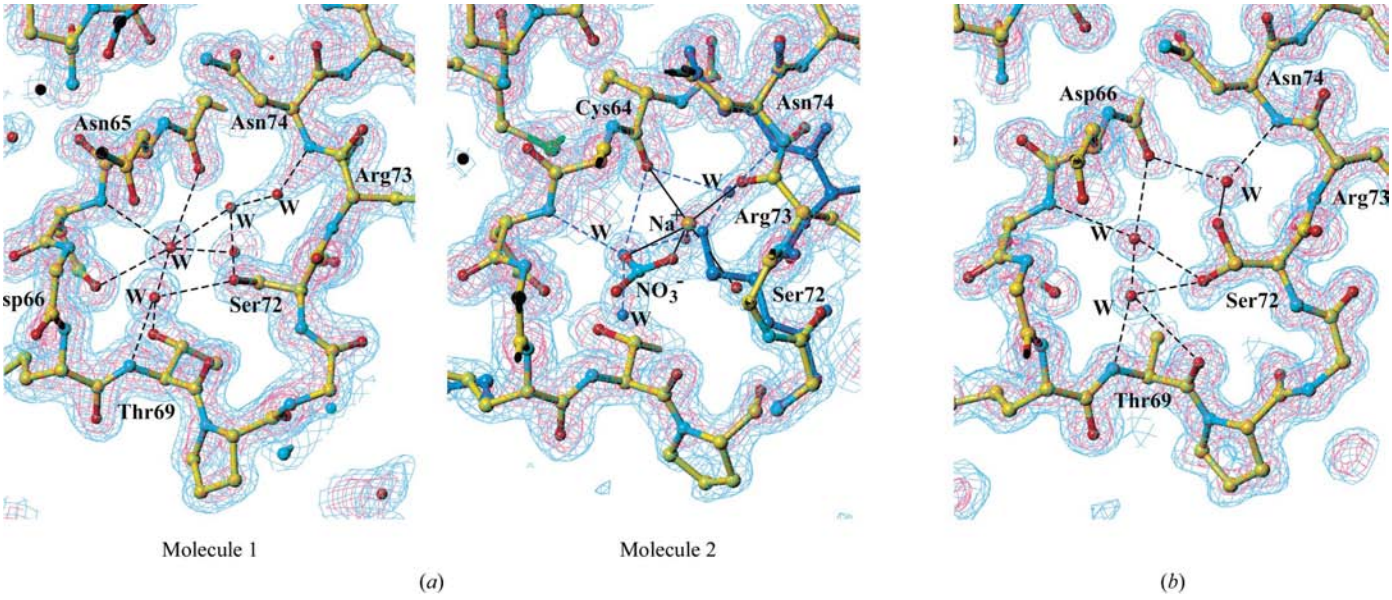

Figure 3
Structures of the loop region Ser60–Leu75 in the type I native crystal (*a*) and transformed crystal (*b*). The region Gly71–Asn74 in molecule 2 is disordered and the water-bound conformer is represented in dark blue. The electron density is drawn at the 1.5σ level (blue) and the 2σ level (red).

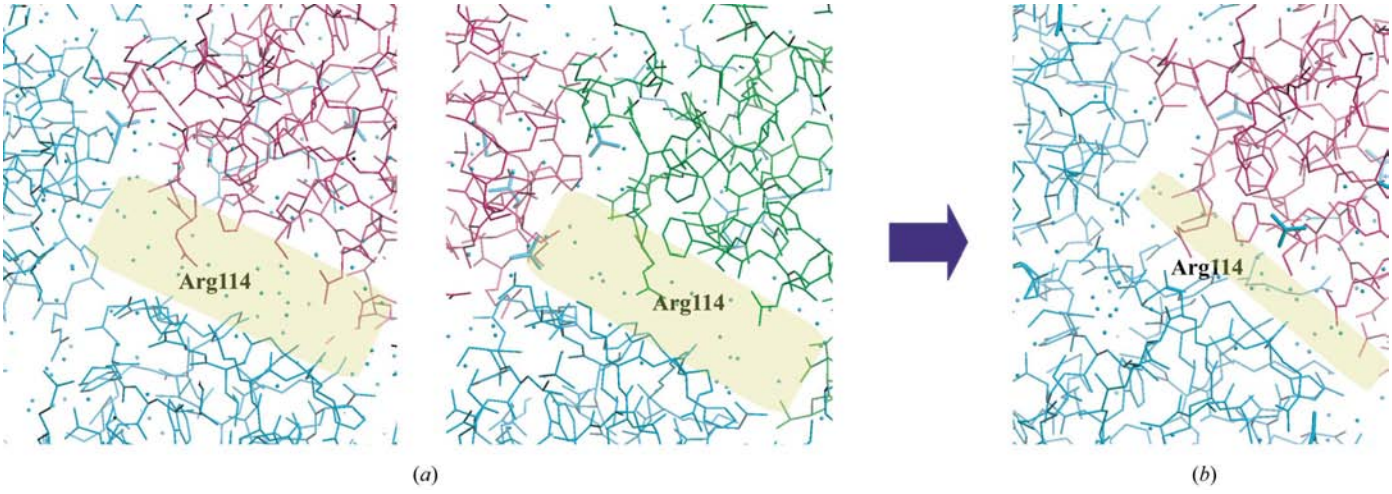

Figure 4
Comparison of the intermolecular contacts between the native type I crystal (*a*) and the transformed crystal (*b*). Two independent molecules in the native crystal are shown in red and green. Symmetry-related adjacent molecules are shown in blue. A bulk-solvent area is denoted by a yellow rectangular box.

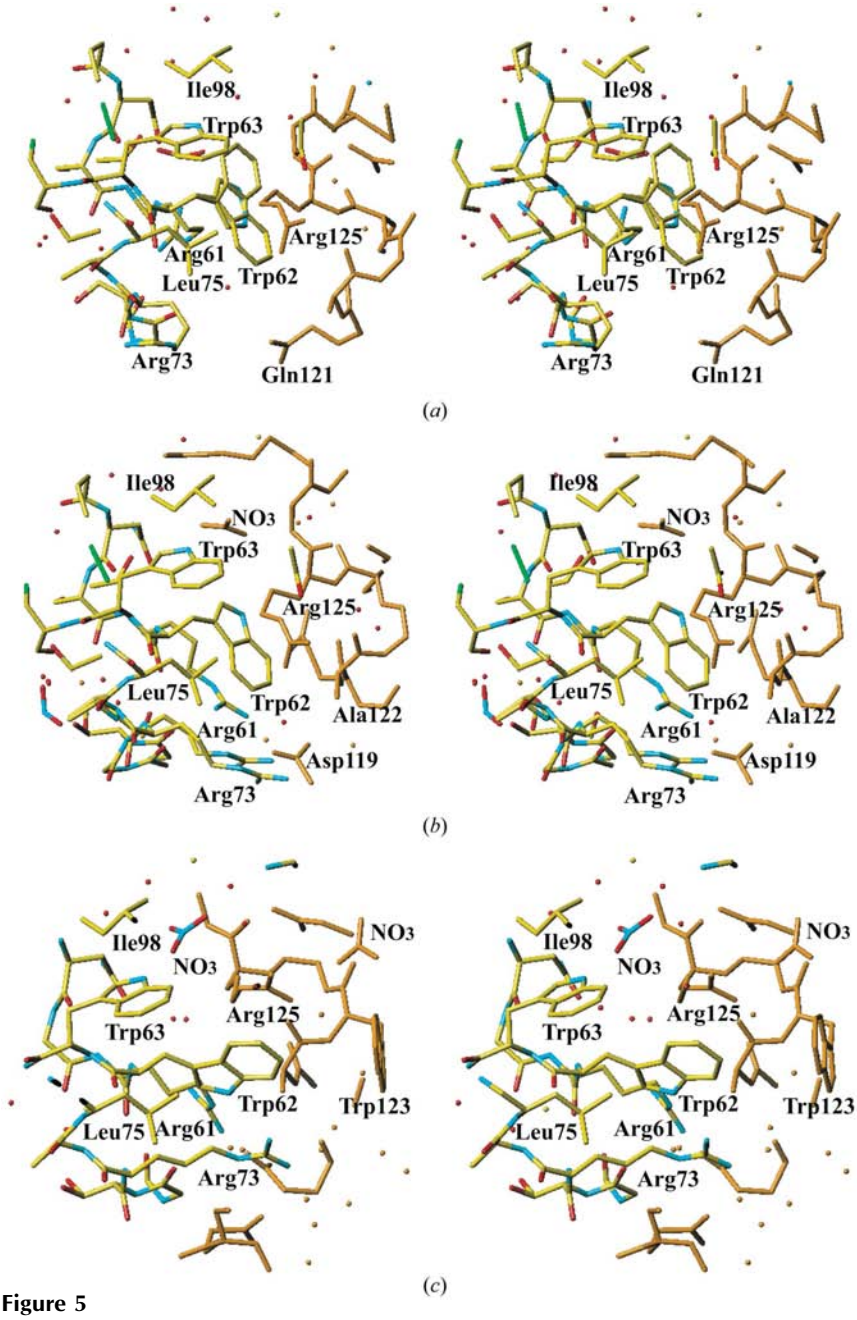

Figure 5
Stereoscopic views of the intermolecular contacts involving Trp62 in molecule 1 (*a*) and molecule 2 (*b*) in the native type I crystal and in the transformed crystal (*c*). Symmetry-related adjacent molecules are rendered in orange.

solvent. In contrast, the side chain of Trp62 in molecule 2 is encapsulated in the intermolecular cleft, with the indolyl group sandwiched between the guanidyl group of Arg61 and the alkyl chain of Arg125 of the adjacent molecule. In the transformed crystal, the side chain of Trp62 is closely packed in the intermolecular cleft. The indolyl group is sandwiched between the guanidyl groups of Arg73 and Arg125 of the adjacent molecule. In addition, the two indolyl groups of Trp63 and Trp123 of the adjacent molecule are in direct contact with and almost perpendicular to the indolyl plane of Trp62, indicating stabilization by the CH–π interaction (Nishio *et al.*, 1998).

3.4. Analysis of the thermal motion

The average u_{eqv} values with their e.s.d.s are given in Table 2. The thermal motions of the two independent molecules in the native crystals are not identical. The average u_{eqv} of molecule 1 is larger than that of molecule 2. On the other hand, the atomic thermal motion of the transformed type I crystal is considerably smaller than the thermal motion in the native crystal. The root-mean-square amplitude of the rigid-body motion is given in Table 2. The rotational amplitude of 1.2° corresponds to about a 0.4 Å shift of atomic coordinates at the edge of the molecule. Therefore, the contribution of the rotational motion to each individual u_{eqv} is comparable to the translational motion on the molecular surface, but the contribution of the translational motion is dominant in the core region of the molecule. The contribution of the rigid-body motion to the atomic u_{eqv} in the type I crystal (33%) is markedly decreased in the transformed crystal (8.7%). The centre of rotation does not coincide with the centre of gravity but is shifted by more than 1 Å. The variation in the shift of the centre of rotation may be ascribed to the fact that the protein molecule in the crystalline state is not a free molecule, but its molecular motion, especially the rotational motion, is restricted by intermolecular contacts.

4. Discussion

4.1. Dehydration and phase transition

Two types of monoclinic crystals of hen egg-white lysozyme, grown under different crystallization conditions, are transformed to a crystal with half the unit-cell volume. The type I crystal is easily transformed to a new crystal by the loss of 41%(*v*/*v*) of the solvent. In contrast, it is hard to dehydrate the type II crystal without deterioration; the phase transition occurs when the solvent loss is 17%. The type II crystal, which was grown in 10%(*w*/*v*) NaCl solution, may contain many more ions than the type I crystal. A change of salt concentration in the crystal influences the protein–solvent interactions and thus affects the dehydration prior to the phase transition. A high concentration of solute ions seems to lower the volatility of water, suppressing evaporation from the crystal.

In our previous paper (Harata & Akiba, 2004), we showed that the phase transition of the triclinic crystal of lysozyme proceeds by way of an intermediate state containing the old lattice of the native crystal and the new lattice of the trans-

Table 2
Summary of the analysis of thermal motion.

Root-mean-square deviations are given in parentheses.

	Type IA		Type IB	Type IIA	
	Molecule 1	Molecule 2		Molecule 1	Molecule 2
Average u_{eqv} values†					
Main-chain atoms (Å^2)	0.25 (0.09)	0.23 (0.08)	0.13 (0.06)	0.29 (0.12)	0.21 (0.08)
All atoms (Å^2)	0.30 (0.16)	0.27 (0.12)	0.16 (0.10)	0.34 (0.17)	0.25 (0.14)
Rigid-body parameters					
R.m.s. rotational amplitude (°)	1.37	1.26	1.17	1.57	1.29
R.m.s. translational amplitude (Å)	0.41	0.40	0.32	0.43	0.38
Shift of the centre of rotation (Å)	2.63	4.12	1.35	4.19	2.44
Rigid-body portion in u_{ij} (%)	33.0	32.9	8.7	10.8	19.4

† u_{eqv} was calculated as the average of three eigenvalues of the u_{ij} tensor.

formed crystal. The present X-ray diffraction analysis has again demonstrated the presence of an intermediate state in the phase transition of the monoclinic crystals. It is a generally accepted concept that protein crystals consist of microcrystals (McPherson, 1999; Drenth, 1999). The change in X-ray diffraction observed during the phase transition can be rationally explained based on the assumption that the structural transformation occurs at the microcrystal level. The phase transition may spontaneously occur in a microcrystal when the solvent content of the microcrystal becomes critical to retaining the packing structure. Once the seed of a new crystal is formed, the transition seems to propagate to neighbouring microcrystals one after another. The gradual decrease in the intensity of $h + l$ odd reflections indicates that the crystal consists of two types of microcrystals in the intermediate state. The diffuse streaks observed in the X-ray diffraction may be caused by less-ordered microcrystals in the interface area between the different types of microcrystals. The increased diffraction power of the transformed crystal indicates that the molecular structure and packing arrangement are much more ordered in the transformed crystal. In contrast to the enhancement of the diffraction power, an unfavourable increase of peak width of diffraction spots is observed in the transformed crystal. The relatively large peak width may be caused by the less-ordered arrangement of microcrystals, indicating that the order of microcrystals does not fully recover after the phase transition.

4.2. Structural changes caused by the phase transition

The backbone structure of the lysozyme molecule in the transformed crystal is essentially the same as the structure in the native crystal. The dehydration induces changes in the crystal packing in which direct contacts between protein molecules are increased because the bulk-solvent region is reduced. In the native crystal, many side-chain groups on the molecular surface protrude into the bulk solvent and some of them show multiple conformations. The disorder is observed in the bulky side-chain groups of Trp62 in molecule 1 and in Arg14, Arg21 and Arg68 in molecule 2, each showing two alternate conformers. In the transformed crystal, these side-chain groups show a single conformation, which is stabilized by intermolecular and/or intramolecular close contacts. Instead, the phase transition caused disorder of the small side-chain groups of Ser72, Ser81 and Ser85. Therefore, the close packing forces the bulky side-chain groups into a single conformation, but the crystal still contains cavity space in which small side-chain groups can retain the conformational flexibility gained in the phase transition.

The two independent molecules in the native type I crystal become equivalent in the transformed crystal. The crystal packing in the native crystal shows that protein molecules are arranged in such a manner as to form a pseudo-*B*-centred lattice (Fig. 1*b*). An obvious deviation from the *B*-centred symmetry is the positional shift along the *b* axis. The difference in the *y* coordinate of the centre of gravity between the two independent molecules is 1.83 Å in the type I crystal. Therefore, the phase transition is a process that adjusts the violation of the *B*-centred symmetry, leading to the formation of a primitive cell with half the volume. The two independent molecules should shift along the *b* axis to cancel the difference in the *y* coordinate. On the other hand, the *b* axis of the transformed crystal is shortened by 4.74 Å in the type I crystal. Therefore, the movement of the two independent molecules is coupled with the shortening of the *b* axis. Such concerted movement in the molecular rearrangement seems to occur in each microcrystal without damaging the crystal, because the type I crystal transformed without crack formation even in samples longer than 1 mm in the *b*-axis direction.

4.3. Sodium-binding site

In the native type I crystal, a sodium ion is partially bound to one of the two independent molecules. On the other hand, each of the two independent molecules fully binds a sodium ion in the type II crystal. The presence of the sodium ion is confirmed by the geometry of the octahedral coordination of ligand O atoms as observed in tetragonal lysozyme crystals (Vaney *et al.*, 1996; Sauter *et al.*, 2001). In molecule 2 of the native type I crystal, the partial binding of the sodium ion accompanies the disorder of the main chain in the region Gly71–Asn74, presenting two alternate conformations: a water-bound form and a sodium-bound form. The corresponding region in molecule 1 shows only the water-bound conformation. The structure of the transformed crystal shows that the sodium-bound conformation in molecule 2 changes to the water-bound form when the sodium and nitrate ions are removed. After the transformation, the peptide group connecting Arg73 and Asn74 in the sodium-bound molecule was rotated 180° around the C^{α}—N bond. Such a rotation of the peptide plane should be associated with the movement of several residues, which may only occur during the rearrangement of the molecules. In contrast to the monoclinic crystal,

the phase transition of the triclinic crystal is associated with the binding of sodium nitrate (Harata & Akiba, 2004). A reversal of the peptide-group orientation was observed in the corresponding loop region where the water-bound form was changed to the sodium-bound form. One reason for the different conformation of the region Gly71–Asn74 in the transformed crystal could be the packing requirement in the transformed crystal. The intermolecular contacts with symmetry-related adjacent molecules may restrict the conformation for better crystal packing.

4.4. Thermal motion and diffraction power

The transformed crystal diffracted to higher resolution than the native crystal. The average u_{eqv} value of the transformed crystal is nearly half that of the native crystal. According to the analysis of the rigid-body motion, the decrease in the atomic thermal motion in the transformed crystal is mostly derived from suppression of the rigid-body motion. The contribution of the rigid-body motion, which is 33% of u_{eqv} for both independent molecules in the native type I crystal, decreases to 8.7% in the transformed crystal, whereas the decrease in the magnitude of the internal part of u_{eqv} is 9.2% for molecule 1 and 14.4% for molecule 2. The prominent decrease of the rigid-body motion in the transformed crystal is mostly attributable to the decrease in the translational motion, which contributes equally to the temperature factor of each atom.

The bulk-solvent area in the crystal is considerably reduced by the dehydration-induced phase transition. As a result, the protein molecules in the transformed crystal, which are densely packed, gain more intermolecular contacts, such as hydrogen bonds and salt linkages, that are formed not only directly but also by mediation of water molecules or ions. The number of intermolecular direct contacts is increased from 13 per molecule in the native crystal to 20 in the transformed crystal. In addition, the increase is prominent in the water-mediated intermolecular contacts. The two protein molecules form 26 water-mediated hydrogen-bond bridges in the native crystal. In contrast, 48 water molecules are involved in forming intermolecular hydrogen-bond bridges in the transformed crystal. Thus, the rigid-body motion in the transformed crystal should be suppressed by the larger number of intermolecular contacts.

This work was supported in part by the New Energy and Industrial Technology Development Organization (NEDO).

References

Bell, J. A. (1999). *Protein Sci.* **8**, 2033–2040.

Dobrianov, I., Caylor, C. L., Lemay, S. G., Finkelstein, K. D. & Thorne, R. E. (1999). *J. Cryst. Growth*, **196**, 511–523.

Dobrianov, I., Kriminski, S., Caylor, C. L., Lemay, S. G., Kimmer, C., Kissekev, A., Finkelstein, K. D. & Thorne, R. E. (2001). *Acta Cryst.* D**57**, 61–68.

Drenth, J. (1999). *Principles of Protein X-ray Crystallography*, 2nd ed., p. 104. New York: Springer–Verlag.

Esnouf, R. M., Ren, J., Garman, E. F., Somers, D. O., Ross, C. K., Jones, Y., Stammers, D. K. & Stuart, D. I. (1998). *Acta Cryst.* D**54**, 938–953.

Harata, K. (1994). *Acta Cryst.* D**50**, 250–257.

Harata, K., Abe, Y. & Muraki, M. (1999). *J. Mol. Biol.* **287**, 347–358.

Harata, K. & Akiba, T. (2004). *Acta Cryst.* D**60**, 630–637.

Kiefersauer, R., Than, M. E., Dobbek, H., Gremer, L., Meloro, M., Strobl, S. & Dias, J. M. (2000). *J. Appl. Cryst.* **33**, 1223–1230.

Kishan, V. R., Chandra, N. R., Sudarsanakumar, C., Suguna, K. & Vijayan, M. (1995). *Acta Cryst.* D**51**, 703–710.

Kodandapani, R., Suresh, C. G. & Vijayan, M. (1990). *J. Biol. Chem.* **265**, 16126–16131.

McPherson, A. (1999). *Crystallization of Biological Macromolecules*, pp. 373–374. New York: CSHL Press.

Madhusudan, Kodandapani, R. & Vijayan, M. (1993). *Acta Cryst.* D**49**, 234–245.

Matthews, B. W. (1968). *J. Mol. Biol.* **33**, 491–497.

Nagendra, H. G., Sudarsanakumar, C. & Vijayan, M. (1996). *Acta Cryst.* D**52**, 1067–1074.

Nagendra, H. G., Sukumar, N. & Vijayan, M. (1998). *Proteins*, **32**, 229–240.

Nishio, M., Hirota, M. & Umezawa, Y. (1998). *The CH/π Interaction.* New York: Wiley–VCH.

Salunke, D. M., Beerapandian, B., Kodandapani, R. & Vijayan, M. (1985). *Acta Cryst.* B**41**, 431–436.

Sauter, C., Otálora, F., Gavira, J.-A. & García-Ruiz, J. M. (2001). *Acta Cryst.* D**57**, 1119–1126.

Sheldrick, G. M. (1997). *SHELXL97. Program for Crystal Structure Refinement.* University of Göttingen, Göttingen, Germany.

Schomaker, V. & Trueblood, K. N. (1968). *Acta Cryst.* B**24**, 63–76.

Sjögren, T., Carlsson, G., Larsson, G., Hajdu, A., Andersson, C., Pettersson, H. & Hajdu, J. (2002). *J. Appl. Cryst.* **35**, 113–116.

Vaney, M. C., Broutin, I., Retailleau, P., Douangamath, A., Lafont, S., Hamiaux, C., Prangé, T., Ducruix, A. & Riès-Kautt, M. (2001). *Acta Cryst.* D**57**, 929–940.

Vaney, M. C., Maignan, M., Riès-Kautt, M. & Ducruix, A. (1996). *Acta Cryst.* D**52**, 505–517.